JPET Fast Forward. Published on March 17, 2010 as DOI: 10.1124/jpet.110.166173

1. TITLE PAGE

A Benzothiophene Inhibitor of MAPK-Activated Protein Kinase 2 (MK2) Inhibits TNFα Production and has Oral Anti-Inflammatory Efficacy in Acute and Chronic Models of Inflammation.

Robert J. Mourey, Barry L. Burnette, Sarah J. Brustkern, J. Scott Daniels, Jeffrey L. Hirsch, William F. Hood, Marvin J. Meyers, Stephen J. Mnich, Betsy S. Pierce, Matthew J. Saabye, John F. Schindler, Sarah A. South, Elizabeth G. Webb, Jian Zhang, and David R. Anderson.

Discovery Biology (R.J.M., B.L.B., S.J.B., J.L.H., W.F.H., S.J.M., M.J.S., J.F.S., E.G.W., J.Z.), Medicinal Chemistry (M.J.M., B.S.P., D.R.A.), Pharmacokinetics, Dynamics and Metabolism (J.S.D., S.A.S), Inflammation Research Unit, Pfizer Global Research and Development, Chesterfield, Missouri

RUNNING TITLE PAGE

Running Title: Benzothiophene MK2 Kinase Inhibitors are Anti-Inflammatory

Corresponding Author:

David R. Anderson

Chemistry Discovery

Pfizer Global Research & Development

Eastern Point Road

Groton, CT 06340

Telephone: 860-686-9254

FAX: 860-686-7842

Email: david.r.anderson@pfizer.com

Number of text pages: 48

Number of tables: 5

Number of figures: 7

Number of references: 40

Number of words in the:

Abstract: 247

Introduction: 746

Discussion: 1440

Abbreviations: MK2, MAPKAP kinase 2; PF-3644022, (10R)-10-methyl-3-(6-methylpyridin-3-yl)-9,10,11,12-tetrahydro-8H-[1,4]diazepino[5',6':4,5]thieno[3,2-f]quinolin-8-one; RA, rheumatoid arthritis; TNF, tumor necrosis factor; IL-1; interleukin-1; MAPKAP, MAPK-activated protein; PRAK, p38-regulated and activated kinase; LPS, lipopolysaccharide; SCW, streptococcal cell wall; MNK, MAPK-interacting kinase; GST, glutathione-S-transferase; MSK, mitogen- and stress-activated protein kinase; FITC, fluorescein isothiocyanate; HSP27, heat shock protein 27; SPR, surface plasmon resonance; hPBMCs, human peripheral blood mononuclear cells; MAPK, mitogen-activated protein kinase; HWB, human whole blood; HPLC, high-performance liquid chromatography; LC-MS/MS, liquid chromatography-tandem mass spectrometry; ELISA, enzyme-linked immunosorbent assay; PK-PD, pharmacokinetic-pharmacodynamic.

Recommended section assignment: Inflammation, Immunopharmacology, and Asthma

3. ABSTRACT

Activation of the p38 kinase pathway in immune cells leads to the transcriptional and translational regulation of pro-inflammatory cytokines. MAPKAP kinase 2 (MK2), a direct downstream substrate of p38 kinase, regulates LPS-stimulated TNFα and IL-6 production through modulating the stability and translation of these mRNAs. Developing small molecule inhibitors of MK2 may yield anti-inflammatory efficacy with a different safety profile relative to p38 kinase inhibitors. This report describes the pharmacologic properties of a benzothiophene MK2 inhibitor [(10R)-10-methyl-3-(6-methylpyridin-3-yl)-9,10,11,12-tetrahydro-8H-[1,4]diazepino[5',6':4,5]thieno[3,2-f]quinolin-8-one; PF-3644022]. PF-3644022 is a potent freely reversible ATP-competitive compound that inhibits MK2 kinase activity (K_i = 3 nM) with good selectivity when profiled against 200 human kinases. In the human U937 monocytic cell line or PBMCs, PF-3644022 potently inhibits TNFα production with similar activity (IC_{50} = 160 nM). PF-3644022 blocks TNFα and IL-6 production in LPS-stimulated human whole blood with IC_{50} values of 1.6 μM and 10.3 μM, respectively. Inhibition of TNFα in U937 cells and blood correlates closely with inhibition of phospho-HSP27, a target biomarker of MK2 activity. PF-3644022 displays good pharmacokinetic parameters in rats and is orally efficacious in both the rat acute LPS-induced TNFα model and the chronic streptococcal cell wall-induced arthritis model. Dose-dependent inhibition of TNFα production in the acute model, and inhibition of paw swelling in the chronic model is observed with ED_{50} values of 6.9 and 20 mg/kg, respectively. PF-3644022 efficacy in the chronic inflammation model is strongly correlated with maintaining a C_{min} greater than the EC_{50} measured in the rat LPS-induced TNFα model.

4. INTRODUCTION

Rheumatoid arthritis (RA) is a chronic inflammatory disease characterized by an imbalance of pro- and anti-inflammatory cytokines, autoimmunity, joint inflammation and eventual joint destruction (McInnes and Schett, 2007). Evidence supporting the role of the pro-inflammatory cytokines TNFα, IL-1β and IL-6 has been demonstrated in both animal models and human clinical trials (Dayer et al., 2001; Scott and Kingsley, 2006; Hennigan and Kavanaugh, 2008). Use of biologic therapeutics that neutralize these cytokines have shown some clinical success in reducing joint pain and inflammation while retarding joint destruction (Smolen and Steiner, 2003). Limits to the use of biologics in RA include high cost of protein pharmaceuticals, parenteral administration, loss of efficacy over time, risk of infection, and a significant portion of patients who show partial or no response to these agents. Therefore, development of orally-active small molecule inhibitors that target signaling pathways regulating inflammatory cytokine production could add significant value to unmet medical need.

In 1994, p38α kinase was identified as a target that regulates inflammatory cytokine biosynthesis (Lee et al., 1994). Since then, kinases have been hotly pursued as drugable targets that regulate inflammation signaling pathways (Gaestel et al., 2007; Gaestel et al., 2009). Activation of the p38 kinase pathway in immune cells leads to the transcriptional and translational regulation of pro-inflammatory cytokine synthesis (Winzen et al., 1999). Many p38 kinase inhibitors have subsequently been developed that demonstrate inhibition of TNFα, IL-1β and IL-6 production and display anti-inflammatory efficacy in animal models (Pettus and Wurz, 2008). In clinical trials, many p38 kinase inhibitors were discontinued due to unacceptable safety profiles, namely

elevated liver enzymes with significant incidence of skin rash (Dominguez et al., 2005). Of the compounds that advanced to testing in RA patients, initial short-term efficacy was observed, but was subsequently lost with further treatment presumably due to feedback control of the p38 kinase network (Hammaker and Firestein, 2010). It is possible, therefore, that other targets upstream or downstream in the p38 kinase pathway may avoid this feedback loop while exhibiting enhanced safety.

Activated p38 kinase directly phosphorylates and activates the mitogen-activated protein kinase-activated protein (MAPKAP) kinases MK2, MK3 and MK5 (also known as PRAK) (Gaestel, 2006). Prior to 1999, it was unclear which downstream p38 kinase pathway components regulated TNFα production. Using $MK2^{-/-}$ knockout mice, TNFα levels were reduced approximately 90% through a post-transcriptional mechanism, demonstrating that MK2 is essential for lipopolysachharide (LPS)-induced TNFα biosynthesis (Kotlyarov et al., 1999). IL-6 and interferon-γ were also significantly reduced, while IL-1 showed only modest reduction (Kotlyarov et al., 1999). MK2 regulates LPS-stimulated TNFα and IL-6 production through modulating the stability and translation of TNF and IL-6 mRNAs via AU-rich elements in the 3'-untranslated region (Neininger et al., 2002). Interestingly, $MK3^{-/-}$ mice showed little reduction in LPS-stimulated TNFα levels while the $MK2^{-/-}MK3^{-/-}$ double knockout exhibited complete inhibition, indicating that MK2 is the major MAPKAP kinase regulating TNFα production (Ronkina et al., 2007). No effect on TNFα synthesis or other cytokines was observed in $PRAK^{-/-}$ mice (Shi et al., 2003) . $MK2^{-/-}$ mice were also resistant to collagen-induced arthritis in a murine model of RA (Hegen et al., 2006). MK2, therefore, is an attractive target for development of anti-inflammatory kinase inhibitors.

The MK2 knockout mouse has been useful in defining MK2's role in inflammation. Having a potent and selective MK2 kinase inhibitor as an investigative tool, however, would be advantageous to further explore the biology of MK2 and the p38 kinase pathway. Potent MK2 inhibitors have been recently described (Anderson et al., 2005; Anderson et al., 2007; Trujillo et al., 2007; Wu et al., 2007; Goldberg et al., 2008; Schlapbach et al., 2008; Xiong et al., 2008; Anderson et al., 2009a; Anderson et al., 2009b; Keminer et al., 2009), but few show nanomolar potency in cells (Schlapbach et al., 2008; Anderson et al., 2009b). Developing potent, selective MK2 inhibitors that have optimized pharmacologic properties for activity in blood or in vivo has been extremely difficult, with just one compound from the pyrrolopyridine series reported to have oral efficacy in blocking TNFα production in LPS-challenged rats (Anderson et al., 2007).

PF-3644022 represents a potent and selective benzothiophene MK2 inhibitor, the first MK2 inhibitor described with oral efficacy in both acute and chronic models of inflammation. This ATP-competitive compound potently inhibits MK2 enzyme activity with good selectivity across 200 human kinases. PF-3644022 potently inhibits LPS-stimulated TNFα production in cells and blood, and when dosed orally in LPS-challenged rats. PF-3644022 exhibits good pharmacokinetic properties demonstrating efficacy in the streptococcal cell wall (SCW)-induced arthritis model.

5. METHODS

Preparation of PF-3644022. PF-3644022, [(10R)-10-methyl-3-(6-methylpyridin-3-yl)-9,10,11,12-tetrahydro-8H-[1,4]diazepino[5',6':4,5]thieno[3,2-f]quinolin-8-one, was prepared by the Pfizer Discovery Medicinal Chemistry Department (Chesterfield, MO) as described (Anderson et al., 2009b). The molecular weight and formula of the parent compound is 374.47 g/mol and $C_{21}H_{18}N_4OS$. The free base form was used for all dosing studies and to calculate solution concentration. Fresh 10 mM PF-3644022 stock concentrations were made in 100% DMSO to support enzyme and cell studies and kept at room temperature for no more than 2 weeks.

Generation of Recombinant Protein Kinases. MAPKAP kinase family recombinant proteins were generated in-house. N-terminally truncated MK2 (amino acids 45-400) was expressed and purified as described (Schindler et al., 2002). To support compound binding studies to MK2, N-terminally-biotinylated MK2 (amino acids 45-371) was expressed in *E. coli* using the BirA expression system (Smith et al., 1998). MK3 (accession #U43784), PRAK (accession #AF032437) and MNK1 (accession #AB000409) were expressed in *E. coli* as glutathione-S-transferase (GST)-fusion proteins and affinity purified over glutathione-sepharose (Amersham Pharmacia Biotech, Piscataway, NJ). The GST-purification tag was removed by thrombin-cleavage and the proteins further purified to homogeneity over Mono Q-sepharaose (Amersham Pharmacia Biotech). The C-terminal kinase domain of MSK1 (amino acids 367-802) (accession #AF074393) and MSK2 (amino acids 351-772) (accession #AJ010119) were expressed as N-terminal 6xHis-tagged fusion proteins in baculovirus-infected *Sf9* insect cells.

MSK1 and MSK2 were purified to near homogeneity over Ni-NTA-agarose (Qiagen, Germantown, MD).

In Vitro Kinase Assays and Inhibition Kinetics. Activated p38α prepared according to (Hope et al., 2009) was used to activate recombinant MAPKAP kinases by incubation at a 1:50 molar ratio with 250 μM ATP for 1 hour at 30°C. The kinase activity of MK2 was followed using fluorescently-labeled heat shock protein 27 (HSP27) peptide (FITC-KKKALSRQLSVAA) and a Caliper LabChip 3000 (Caliper Life Sciences, Hopkinton, MA). Phosphorylated peptide was separated from substrate peptide electrophoretically and quantified. All kinase reactions were performed at room temperature in 20 mM HEPES, containing 10 mM $MgCl_2$, 1 mM DTT, 0.01% BSA, and 0.0005% Tween-20, pH 7.5. Unless specified otherwise, the reactions were initiated by the addition of enzyme. For endpoint experiments, reactions were terminated during the linear phase by the addition of 30 mM EDTA. The kinase selectivity experiments were performed with the MgATP concentration fixed at the $K_{m(app)}$ determined for each enzyme.

To determine the mechanism of action of PF-3644022 binding, the initial velocities in the presence and absence of PF-3644022 with ATP as the varied substrate while the HSP27 peptide concentration was held constant. The data were fit to the competitive inhibition model (equation 1), noncompetitive inhibition model (equation 2) or an uncompetitive inhibition model (equation 3). In these equations, V_{max} is the maximum velocity, K_m is the Michaelis –Menton constant for the varied substrate, S is the concentration of the varied substrate, I is the concentration of the inhibitor, and K_{is} and K_{ii} are the slope and intercept inhibition constants, respectively. The best fit was

based on an F-test and resulted in the lowest standard errors for the inhibition constants. The apparent inhibition constants (K_i) were determined using GraFit 5.0 (Leatherbarrow, 2001).

equation 1: $v = V_{max} * S / (K_m * (1+I/K_{is}) + S)$

equation 2 $v = V_{max} * S / (K_m * (1+I/K_{is}) + S * (1+I/K_{ii}))$

equation 3 $v = V_{max} * S / (K_m + S * (1+I/K_{ii}))$

Other MAPKAP enzymes were assayed for activity using an ion exchange separation method for the detection of ^{33}P-labeled product peptide as described (Anderson et al., 2007). PF-3644022 was evaluated for inhibition of 200 human kinases using an in-house 30 kinase selectivity panel (Card et al., 2009) and 170 kinases from the Upstate Kinase Profiler service (Millipore, Bedford, MA). The kinase selectivity experiments were performed with the MgATP concentration fixed at the $K_{m(app)}$ determined for each enzyme.

MK2 Inhibitor Binding Studies. Surface plasmon resonance (SPR) spectroscopy employing standard Biacore methodology on a Biacore 3000 instrument (GE Healthcare, Piscataway, NJ) was used to follow real-time binding kinetics of PF-3644022 to immobilized biotinylated MK2. The binding studies were performed at 25°C using a running buffer of 10 mM HEPES, 150 mM NaCl, 0.005% P20 detergent with a flow rate of 60 µl/min. PF-3644022 (1-100 nM) was injected over immobilized MK2 for 4 min and then dissociation followed for 15 min. For biotin-MK2 capture, a CM5 chip (Biacore, Piscataway, NJ) was first pre-conditioned and then streptavidin immobilized using amine coupling with N-hydroxysuccinimide and N-ethyl-N'-(3-dimethylaminopropyl) carbodiimide according to Biacore methods. For kinetic analyses,

sensorgrams were double reference subtracted and BiaEvaluation (Biacore) used to determine the association and dissociation constants using a Langmuir 1:1 model.

Cell-Based Assays. The U937 human premonocytic cell line was obtained from the American Type Culture Collection (Rockvile, MD) and differentiated to a monocyte/macrophage phenotype with phorbol myristate acetate (Sigma Chemical, St. Louis, MO) as described (Burnette et al., 2009). Human peripheral blood mononuclear cells (hPBMCs) were prepared from venous blood of donors collected anonymously with informed consent at an on-site clinic. Venous blood was collected into sodium heparin tubes and hPBMCs isolated by density gradient centrifugation using Histopaque 1077 (Sigma Chemical) as per manufacturer's directions. U937 cells and hPBMCs were cultured as described (Burnette et al., 2009; Hope et al., 2009).

The ability of PF-3644022 to inhibit LPS-stimulated cytokine production in U937 cells and hPBMCs was evaluated following a 1 hr pre-treatment of compound in cell culture media containing less than 1% DMSO final concentration. All cell incubations were done at 37°C. Culture media TNFα levels were measured 4 hr following LPS-stimulation at 100 ng/ml using an electrochemoluminescence MesoScale Discovery TNFα kit (MesoScale Discovery, Gaithersburg, MD). In hPBMCs, TNFα, IL-1, IL-6 and IL-8 were measured at 16 hr following LPS-stimulation using a 4-plex human cytokine MSD plate (MesoScale Discovery). For mitogen-activated protein kinase (MAPK) signaling studies in U937 cells, cells were pretreated with PF-3644022 at varying concentrations for 1 hr prior to LPS stimulation at 100 ng/ml for 30 min. Cell lysates were prepared and analyzed for phospho-Ser78-HSP27, phospho-p38 and phospho-JNK levels by Western blot analysis as described (Anderson et al., 2007).

Quantitation of Western blots was performed using Alexa-conjugated secondary antibodies (Invitrogen, Madison, WI) and fluorescent LICOR (LICOR Biosciences, Lincoln, NE) scanning. MK2 activity in U937 cells, measured by monitoring the phosphorylation of the MK2 substrate HSP27, was quantitated in cell lysates using a phospho-Ser82 HSP27 and total HSP27 MSD kit. Phospho-HSP27 levels were normalized in cell lysates to total HSP27 protein levels.

LPS-Stimulated Human Whole Blood. Venous blood from human donors was collected in sodium heparin tubes (Baxter Healthcare, Deerfield, IL) and assayed for LPS-stimulated cytokine production as described (Burnette et al., 2009). In brief, PF-3644022 was added to human whole blood (HWB) ex vivo 1 hr prior to stimulation with 100 ng/ml LPS at 37°C. TNFα was measured 4 hr post-stimulation by assaying plasma with a human TNFα MSD kit. TNFα, IL-1, IL-6 and IL-8 in plasma was also measured after 16 hr LPS stimulation of HWB using a 4-plex human cytokine MSD plate (MesoScale Discovery). MK2 activity in HWB was measured by monitoring phospho-Ser82 HSP27 and total HSP27 levels following a 30 min stimulation of 100 ng/ml LPS using a Dissociation-Enhanced Lanthanide Fluorescent Immunoassay (DELFIA; Perkin Elmer, Waltham, MA) as described (Burnette et al., 2009).

Measurement of PF-3644022 in Plasma. Plasma was analyzed for total PF-3644022 by a high-performance liquid chromatography (HPLC) method. In brief, calibration standards ranging from 0.27 nM to 13 μM were prepared by fortifying appropriate amounts of PF-3644022 to blank control plasma by a series of dilutions. Samples and calibration standards were briefly vortex-mixed and 0.025 ml aliquots were transferred from the vials into corresponding 96-well plates. Internal standard working

solution (0.25 μM tolbutamide in 97.5% methanol/ 2.5% acetonitrile containing 1% formic acid) was then added as a 0.225 ml aliquot to all samples. The plates were centrifuged at approximately 3800 rpm for 5 min. A total of 90 μl of supernatant were transferred to a new 96-well TomTec Quadra 96-320 automatic sample handling system (Hamden, CT, USA). The samples (5 μl) were injected onto the liquid chromatography-tandem mass spectrometry (LC-MS/MS) system for analysis. Samples were chromatographed with a Rheos pump (Thermo Fisher Scientific, USA) and an Extend C18 (20 mm x 2.1 mm, 5 μm particle size) column (Agilent, Santa Clara, CA) connected to a HTS-PAL autosampler from Leap Technologies (Carrboro, NC). The mobile phases were 10 mM ammonium acetate in 95% water / 5% methanol (A) and 10 mM ammonium acetate in methanol (B). The running condition was 70% A for 0.5 min isocratically, ramped to 100% B in 1 min, holding for 0.9 min followed by dropping to 30% B in 0.1 min and holding at 30% B another 0.5 min before the next injection. The total run time was 3 min. The HPLC flow rate was maintained at 0.4 ml/min for the entire analysis. An API 4000 triple quadruple mass spectrometer (AB/MDS-Sciex, Concord, Ont., Canada) with a turbo-ionspray interface operated in positive ionization mode was used for the multiple reaction monitoring LC-MS/MS analyses. The mass spectrometric conditions were optimized for detection of PF-3644022 and tolbutamide. The following precursor product ion transitions were used for multiple reaction monitoring: PF-3644022: *m/z* 375 → 291 and tolbutamide, *m/z* 271 → 155, respectively.

LPS-Induced TNFα Production in Rats. All rat in vivo studies were reviewed and approved by the Pfizer Institutional Animal Care and Use Committee according to guidelines sanctioned by the Association for Assessment and Accreditation of Laboratory

Animal Care, International. In the LPS-induced acute endotoxemia inflammation model, adult male Lewis rats (225-250 g; Harlan, Indianapolis, IN) were fasted 18 hr prior to oral dosing and allowed free access to water. PF-3644022 was prepared as a suspension in a vehicle consisting of 0.5% methylcellulose (Sigma Chemical), 0.025% Tween 20 (Sigma Chemical) in water. PF-3644022 or vehicle was orally administered in a volume of 1 ml using an 18-gauge gavage needle 4 hr prior to LPS challenge. LPS was administered by injection into the penile vein at 1 mg/kg in 0.5 ml sterile saline and blood was collected 90 min later by cardiac puncture. Serum TNFα levels were measured using a rat TNFα enzyme-linked immunosorbent assay (ELISA) (Burnette et al., 2009) and PF-3644022 levels determined by LC-MS/MS.

Streptococcal Cell Wall-Induced Arthritis in Rats. Arthritis was induced in 125-140 g female Lewis rats (Harlan) by a single intraperitoneal injection of peptidoglycan-polysaccharide complexes from group A streptococcal cell wall (SCW) purchased from Lee Laboratories (Grayson, GA) as described (Hope et al., 2009). The disease course is biphasic with an acute inflammatory non-T cell dependent phase on days 1-3 followed by a chronic T cell-dependent inflammatory-erosive arthritis developing over days 14-28. Animals developing the acute inflammatory phase were pooled into groups of 7-8 animals per group and dosed with PF-3644022 or methylcellulose-Tween-20 vehicle by oral gavage (1 mL) twice a day for days 10-21. Hind paw swelling volumes were measured on day 21 using a displacement plethysmometer. After the last PF-3644022 dose on day 21, plasma was collected at various times up to 11 hr to determine compound exposure parameters.

Determination of In Vivo Rat Pharmacokinetic Parameters of PF-3644022.

Male Sprague-Dawley rats weighing 275 to 300 grams were purchased from Charles River Laboratories (Wilmington, DE) and acclimated to their surroundings for approximately one week with food and water provided ad libitum. A minimum of one day prior to study, animals were anesthetized with Isoflurane (to effect) and then implanted with Culex (BASi, West Lafayette, IN) vascular catheters in the carotid artery. Animals were acclimated in Culex cages overnight prior to dosing. Patency of the carotid artery catheter was maintained using the "tend" function of Culex ABS. PF-3644022 was administered dissolved in 70% normal saline/20% polyethylene glycol-400/10% ethanol (i.v.) or suspended in 0.5% hydroxypropylmethylcellulose/0.1% Tween 80 in distilled water (p.o.). Blood collections were obtained from the carotid artery and performed by the Culex at 2 (i.v. only), 5, 15, 30 minutes and 1, 2, 4, 6, 8, 12, 18, and 24 hours. Plasma was separated and frozen for analysis.

Concentrations below the limit of quantitation (BLQ) were reported as zero (0) and were used in the evaluation of mean concentrations and the estimation of AUC. The peak plasma concentration (C_{max}) and the time to reach peak concentration (T_{max}) were recorded directly from individual plasma concentration-time profiles. The terminal log-linear phase of the plasma concentration-time curve was identified by linear regression of data points, which yielded an R-squared value. The terminal half-life (t½) was calculated as ln(2) divided by absolute value of the slope of the terminal log-linear phase. The area under the plasma concentration-time curve from time zero to time of the last quantifiable concentration (t) (AUC_{0-t}) was determined using the linear trapezoidal method. The area under the plasma concentration-time curve from time zero to infinity ($AUC_{0-\infty}$) was

determined as AUC_{0-t} plus the extrapolated area. The extrapolated area was determined by dividing the last observed plasma concentration by the slope of the terminal log-linear phase. The initial plasma concentrations (C_0) following IV dosing were extrapolated from the apparent distribution phase for individual animals following IV administration. Systemic plasma clearance (CLp) was calculated as dose/ $AUC_{0-\infty}$ while the volume of distribution at steady state (Vd_{ss}) was calculated as CL × MRT, where MRT (mean residence time) was defined as $AUMC_{0-\infty}/AUC_{0-\infty}$. The absolute oral bioavailability (F) was then calculated as a ratio of the mean dose-normalized AUC (0-t or 0-∞) following PO administration to the mean dose-normalized AUC (0-t or 0-∞) following IV administration. The extent of binding of PF-3644022 to rat and human plasma was determined in vitro using an ultracentrifugation method as described (Burnette et al., 2009).

6. RESULTS

The MK2 Inhibitor PF-3644022 is Competitive with ATP and Displays Good Selectivity Across the Human Kinome. Compounds from the benzothiophene series were identified in a Pfizer compound library screen showing both potent MK2 inhibitory activity and good cellular potency at blocking LPS-stimulated TNFα production (Anderson et al., 2009a). Modifying the hinge binding element of the scaffold as well as adding selectivity-promoting substituents led to further increases in MK2 enzyme potency and cellular activity, while enhancing kinase selectivity and oral bioavailability (Anderson et al., 2009b). The structure of our lead compound, PF-3644022, is shown in Fig.1. PF-3644022 in DMSO stock solutions was shown to lose activity over time. Analysis by LC-MS/MS showed that the compound contained significant oxidation of the thiophene ring by 4 weeks in DMSO at room temperature (data not shown). PF-3644022, however, was stable in aqueous solutions with undetectable levels of oxidation after 4-8 weeks. Therefore, PF-3644022 was solubilized in DMSO and used immediately to support analytical, enzyme and cell studies.

PF-3644022 inhibits recombinant MK2 kinase activity with an IC_{50} value of 5.2 nM (Table 1). Additional characterization of PF-3644022 showed that it is competitive versus MgATP with a competitive inhibition constant of 3.0 nM (Fig. 2A and Table 1). The competitive inhibition versus MgATP is apparent in the plot (Fig. 2B) which shows a family of lines intersecting on the 1/v axis, indicative of competitive inhibition. Given that a number of studies have demonstrated that the structure of the ATP binding sites of protein kinases can be effected by the phosphorylation state, we also determined the binding kinetics of PF-3644022 against the nonphosphorylated form of MK2 using SPR.

Rapid association and dissociation kinetics were observed for PF-3644022 binding to nonphoposphorlyted MK2 (Table 1). Taken together these rate constants provide a K_d value of 5.9 nM, which is similar the competitive inhibition constant determined with the phosphorylated form of MK2. Enzyme kinetic studies and crystallographic analyses performed with MK2 supports that PF-3644022 binds in the MK2 ATP pocket (Anderson et al., 2009a; Anderson et al., 2009b).

The inhibitory activity of PF-3644022 against other MAPKAP kinase family members was evaluated as described under *Methods*. At K_m levels of ATP for each kinase, PRAK is inhibited with equivalent potency as MK2, while close family member MK3 has an IC_{50} of 53 nM, about 10-fold weaker (Table 1). Other than MNK2 with an IC_{50} of 148 nM, other family members were largely not inhibited showing at least several hundred-fold selectivity versus MK2. Although PF-3644022 is an ATP-competitive kinase inhibitor, it displays good selectivity against a diverse panel of 200 human kinases tested at K_m levels of ATP (*Supplementary Table 1*). Of the 200 kinases tested for percent inhibition with 1 μM PF-3644022, 16 kinases showed greater than 50% inhibition. These kinases were further profiled to generate IC_{50} values (Table 2). Of the 16 kinases examined for IC_{50} values, 13 kinases were less than 100-fold selective and nine kinases showed less than 25-fold selectivity versus MK2. Ten of the 16 kinases that PF-3644022 inhibited were not surprisingly, members of the CAMK group where MK2 resides. One or two other kinases representing the CMGC, STE, TK and TKL groups were also inhibited by PF-3644022 (Table 2). More importantly, excluding MK3 and MNK2 which may contribute a minor component to TNFα production, other potential TNFα-

regulating kinase targets such as ERKs, IKKs, JNKs, MEKs, MKKs and p38α/β were not significantly inhibited by PF-3644022 (*Supplementary Table 1*).

PF-3644022 Blocks LPS-Stimulated TNFα Production in Cells and Whole Blood. TNFα production induced by LPS-stimulation in the U937 monocytic cell line was measured four hr after LPS addition which was previously shown to coincide with peak TNFα levels in cell culture. PF-3644022 blocked LPS-induced TNFα production with an IC_{50} of 159 nM (Table 3, Figure 3). The effect of PF-3644022 on phosphorylation of MAPK pathway members as well as MK2 activity measured by phosphorylation of HSP27 was quantitated in U937 cell lysates generated after stimulating cells with LPS for 30 min. PF-3644022 had little effect on blocking p38α or JNK1/2 phosphorylation while inhibiting phospho-Ser78-HSP27 levels with a similar concentration-response as TNFα production (Fig. 3A). ERK and c-jun phosphorylation levels were also unchanged by PF-3644022 treatment (data not shown). Inhibition of MK2 activity as measured by inhibition of phospho-Ser82 HSP27 levels indicates an IC_{50} of 201 nM (Table 3). These data show that TNFα inhibition in LPS-stimulated U937 cells correlates with inhibition of MK2 activity and not inhibition of other MAPK pathway targets implicated in TNFα production.

In addition to the U937 cell line, PF-3644022 inhibits TNFα production in hPBMCs and HWB. Inhibition by PF-3644022 in hPBMCs is similar to U937 cells (Figure 3B), with an IC_{50} of 160 nM (Table 3). Interestingly, the cellular inhibition of TNFα production and MK2 activity is approximately 30-fold weaker than in the MK2 enzyme assay, perhaps due to competition by much higher cellular ATP levels. TNFα inhibition in LPS-stimulated HWB is further right-shifted with an IC_{50} of 2 μM, which

correlates nicely with inhibition of MK2 activity measured in HWB lysates (Table 3). The lower potency of PF-3644022 in HWB can be rationalized by factoring in the measured human plasma protein binding of 93.6% (data not shown), resulting in an unbound concentration or free fraction IC_{50} of 126 nM, similar to the PF-3644022 potency in U937 and hPBMCs. Furthermore, the potency of PF-3644022 in cell culture can be right shifted with increasing amounts of serum (data not shown). The effect of PF-3644022 on other pro-inflammatory cytokines IL-1β and IL-6, as well as the chemokine IL-8, was explored in LPS-stimulated hPBMCs and HWB (Fig. 4). Inhibition of IL-1β, IL-6 and IL-8 levels by PF-3644022 in hPBMCs is observed (Fig 4A), albeit with approximately 10-fold weaker IC_{50} values of 1-2 μM relative to TNFα inhibition (Table 3). Although the concentration-response curves have steep slopes between 1-5 μM, no cell toxicity is detected up to 20 μM PF-3644022 (data not shown). The inhibition of LPS-stimulated IL-6 production by PF-3644022 in HWB is similarly 10-fold right shifted as in hPBMCs, with an IC_{50} of 10 μM (Figure 4B, Table 3). Interestingly, in HWB, IL-8 and IL-1β are weakly inhibited by PF-3644022 (Figure 4B).

PF-3644022 Inhibits TNFα Production in the Acute LPS-Challenged Rat Model. Although many benzothiophene inhibitors exhibit submicromolar potency in cells, very few have sufficient pharmacokinetic properties to support in vivo evaluation or activity. The pharmacokinetic parameters measured for PF-3644022 in rats are shown in Table 4. PF-3644022 shows good oral bioavailability and is rapidly absorbed in suspension dosing with a T_{max} of 0.17 hr, a good volume of distribution and terminal half-life of 9.1 hr. Clearance of PF-3644022 from circulating rat blood is also reasonably low. The exposure and pharmacokinetic parameters of PF-3644022 at a 3 mg/kg

suspension dose suggests that PF-3644022 may have sufficient properties to support in vivo evaluation of anti-inflammatory efficacy in rat models.

The oral efficacy of PF-3644022 was evaluated in the acute LPS-challenged rat model. Single doses of PF-3644022 ranging from 0.2 mg/kg to 60 mg/kg were given to Lewis rats as an oral suspension in methacellulose-Tween vehicle 4 hr prior to LPS-challenge. Intravenous administration of LPS to Lewis rats produces a rapid and transient elevation of TNFα levels in plasma that peaks 1-2 hr after LPS injection. TNFα and compound levels in the rat plasma were measured 90 min after LPS injection. Oral dosing of PF-3644022 yields a nice dose-dependent response (Fig. 5A) for TNFα inhibition with an ED_{50} and ED_{80} of 6.9 and 19 mg/kg, respectively (Table 5). This corresponds to an EC_{50} and EC_{80} of 1.4 and 4.2 μM total concentration of PF-3644022 5.5 hr after an initial oral dose (Fig. 5B, Table 5). The EC_{50} in the rat acute LPS-challenge model is similar to PF-3644022 activity in HWB (Table 3) and when corrected for rat plasma protein binding (92.1%), the unbound free fraction EC_{50} is 110 nM (Table 5), again correlating well with TNFα inhibition in U937 cells and hPBMCs (Table 3). The pharmacokinetic and pharmacodynamic (PK-PD) response of TNFα inhibition in the endotoxin-stimulated rat model was examined up to 36 hr following a single ED_{80} oral dose of PF-3644022 (Fig. 5C). For each timepoint where plasma PF-3644022 levels are measured, that group of rats is injected with LPS 90 min prior to blood collection. A nice mirrored response is seen between PF-3644022 and TNFα levels over time, with minimal TNFα production observed at maximal PF-3644022 plasma levels. Maximal TNFα response returns as compound is cleared from the blood, demonstrating an immediate and reversible pharmacodynamic response to MK2 inhibition in this model.

PF-3644022 Suppresses Chronic Inflammation in the Streptococcal Cell Wall-Induced Arthritis Rat Model. The rat SCW model is characterized by a biphasic inflammation response with an acute phase on days 1-5 followed by a more severe and chronic inflammation phase from days 10-21. In the acute phase, hemorrhage and fibrin deposition in the joint synovial space occurs with the accumulation of activated macrophages in the soft tissue. In the more severe chronic phase, intense cell infiltration, joint inflammation and bone destruction in the rat paw is observed. TNFα and IL-1β play a role in the disease process as neutralizing antibodies to these cytokines show the ability to attenuate the disease (Kuiper et al., 1998). PF-3644022 shows dose-dependent inhibition of chronic paw swelling measured on day 21 following 12 days of oral dosing b.i.d. (Fig 6A). The observed ED_{50} for PF-3644022 is 20 mg/kg, while the ED_{80} could only be estimated to be 50-100 mg/kg because maximal efficacy for MK2 inhibition appears to plateau at approximately 80% inhibition in this model (Table 5). At calculated EC_{50} and EC_{80} PF-3644022 concentrations in rat plasma, the mean C_{max} and C_{min} values are 11 and 0.91 μM, respectively (Table 5). Interestingly, the C_{min} at EC_{50} in the chronic rat SCW model is similar to the EC_{50} for TNFα inhibition in the acute rat LPS-model, suggesting that efficacy may be driven by C_{min}. This finding is also reinforced when evaluating the exposure-time response generated at various doses in the rat SCW experiment #3 on day 21 (Fig. 6B). At efficacious doses generating greater than 50% inhibition of paw swelling, the C_{min} must exceed the rat LPS EC_{50} for TNFα inhibition for nearly the entire dosing period. In other words, at least 50% of MK2 activity must be inhibited at all times for an MK2 inhibitor to be efficacious in the rat SCW chronic arthritis inflammation model.

The Pharmacologic Profile of the MK2 Inhibitor PF-3644022 Strongly Links TNFα Inhibition with Efficacy in Acute and Chronic Models of Inflammation. The potency and efficacy of PF-3644022 was compared across in vitro and in vivo assays, including recombinant human MK2 activity, LPS-induced TNFα production in U937 cells, hPBMCs, HWB, and efficacy in rat acute and chronic models of inflammation. When inhibition is plotted against PF-3644022 concentrations, using unbound free fraction plasma levels in the case of ex vivo or in vivo studies, there is very good correlation between compound concentration and efficacy (Fig. 7). Inhibition of TNFα production in cells through direct inhibition of MK2 enzyme activity leads to efficacy in rat acute and chronic models of inflammation. The composite EC_{50} value for these studies is 139 nM (Fig. 7). This is the minimum unbound plasma concentration needed to inhibit greater than 50% cellular activity for TNFα production, and may represent a C_{min} needed for efficacy in chronic inflammatory disease. The close correlation observed in these assays allows an initial prediction of the exposures that may be required for efficacy in human TNFα-mediated inflammatory diseases.

7. DISCUSSION

When it was reported that MK2 is essential for LPS-stimulated TNFα production (Kotlyarov et al., 1999), many pharmaceutical companies who had ongoing p38 kinase programs initiated MK2 projects as alternate approaches to modulating the p38 kinase pathway. Although numerous screening campaigns were run, initial leads were sparse, highly promiscuous, and lacked cell activity. Although several different crystal forms of MK2 were generated by us and other groups, it is extremely difficult to obtain high diffracting data sets, thus limiting the application of structure-based drug design. Of the MK2 structures that were solved, MK2 was shown to have a narrow and deep ATP-binding cleft (Anderson et al., 2007; Hillig et al., 2007; Anderson et al., 2009a; Anderson et al., 2009b). Because of this narrow cleft, MK2 inhibitors need to be mostly planar to bind to the ATP pocket. Typical approaches of optimizing selectivity by appending substituents out of the binding plane was not readily applicable to MK2 inhibitors. Most kinase inhibitors bind to the ATP pocket through a nitrogen-containing ring or element that binds to the kinase hinge region and another interaction gained through hydrogen bonding with the conserved catalytic Lys or Asp of the activation loop. The nitrogen atom of the polyaromatic core forms a hydrogen bond to the hinge and the 4-methyl-3-pyridinyl group of PF-3644022 imparts selectivity against other kinases (Anderson et al., 2009b). The configuration of the stereogenic center on the lactam ring is important for potency and the lactam carbonyl is required for interactions with the conserved catalytic Lys and activation loop Asp.

In this report we refer to PF-3644022 as a selective MK2 inhibitor. In actuality, PF-3644022 is a MK2/MK3/PRAK inhibitor. PRAK is inhibited with equal potency to

MK2 while MK3 is approximately 10-fold weaker (Table 1). While no structure of PRAK has been reported, the structure of MK3 recently has (Cheng et al., 2009). The structures of MK2 and MK3 superimpose well, but there are slight differences between MK2 and MK3 noted in the ATP binding pocket. MK2 Leu141 is replaced with slightly larger Met121 in MK3, whose side chain protrudes at the bottom of the adenine pocket. Perhaps this modification or others are responsible for the 10-fold weaker inhibition of MK3 activity by PF-3644022. Based on $MK2^{-/-}$, $MK3^{-/-}$ and $MK2^{-/-}MK3^{-/-}$ mouse studies, inhibition of LPS-stimulated TNFα synthesis is predominantly through MK2. Even with a MK2/MK3/PRAK inhibitor, PF-3644022 will inhibit a subset of substrates in the p38 kinase pathway and may offer advantages to the more global effects of a p38 kinase inhibitor. Additionally, PF-3644022 inhibits seven other CAMK superfamily members with less than 100-fold selectivity, as well as a scattering of four other kinases across the human kinome (Table 2). None of these other kinases are implicated in TNFα production. PF-3644022 is the most selective MK2 inhibitor described to date.

Of the MK2 inhibitor chemotypes reported, few have submicromolar potency at inhibiting TNFα production in cells, perhaps due to poor physiochemical properties, poor cell permeability, poor biochemical efficiency (BE) (ratio of binding affinity to target versus cellular activity), or inadequate enzyme potency. Of several MK2 chemotypes investigated within Pfizer, only the benzothiophenes have cellular IC_{50} values less than 500 nM. PF-3644022 is a highly permeable and potent MK2 inhibitor (K_i = 3 nM), yet exhibits poor BE with at least 30-fold weaker activity at inhibiting TNFα production in cells (Table 3). Given that PF-3644022 is an ATP competitive inhibitor, the shift in cellular potency may be due to competition with high cellular concentrations of ATP (~5

mM). We have determined that the binding constant of MgATP for non-active MK2 is 30 μM (data not shown). The high affinity of non-active MK2 for ATP is in contrast to the very low affinity of ATP for non-active p38 (>10 mM). The observation that most ATP competitive p38 MAPK inhibitors bind with similar affinity to both the activated and non-activated kinase while MgATP strongly prefers the phosphorylated, active form of p38 kinase suggests that p38 kinase inhibitors will maintain enzyme potency in cellular systems (Schindler et al., 2007).

Additional increases in MK2 inhibitor BE may be achieved through further increases in K_i, tight binding slow off-rate kinetics, non-competitive, uncompetitive or irreversible mechanisms. We believe that the best K_i values achievable with MK2 are low nM, as we were unable to achieve further potency even after gaining additional interactions in the ATP pocket. We also developed several irreversible MK2 inhibitors as tool compounds that did in fact exhibit BEs near 1, but had insufficient selectivity to explore as drug leads. In several MK2 screening campaigns, non-competitive or "allosteric" leads were never identified, and to date, none have been reported by others. In a BE analysis of 50 marketed drugs (Swinney, 2004), 76% had BEs greater than 0.4. For PF-3644022, the calculated BE is 0.03, similar to statin drugs. Swinney concluded that the lower the BE, the more drug would be required for efficacy and the lower the therapeutic index, with higher incidence of toxicity. Although the MK2 knockout mouse validated MK2 as a very attractive target for TNFα inhibition, the very low BE suggests low probability of success developing MK2 inhibitors as drugs.

Achieving activity in whole blood with MK2 inhibitors has been very challenging, possibly due to high plasma protein binding (e.g. >98%). The measured plasma protein

binding for PF-3644022 was 93.6% and 92.1% in human and rat blood, respectively, providing sufficient unbound concentrations to display activity in blood. In LPS-stimulated human monocytes or HWB, p38 kinase inhibitors show nearly equivalent potency in blocking TNFα, IL-1β and IL-6 through regulating cytokine production at both a transcriptional and post-transcriptional level (Burnette et al., 2009; Hope et al., 2009). In LPS-stimulated hPBMCs, PF-3644022 blocks these cytokines as well, although approximately 10-fold more active at inhibiting TNFα (Table 3). In LPS-stimulated HWB, however, PF-3644022 predominantly inhibits TNFα while IL-6 inhibition is 10-fold weaker (Table 3). Little to no inhibition of IL-1β or IL-8 is seen up to 25 μM. These results are consistent with MK2 regulating TNFα and IL-6 through a post-transcriptional mechanism, primarily through modulating the stability and translation of TNFα and IL-6 mRNA (Neininger et al., 2002). The ability of MK2 inhibitors to preferentially block TNFα, IL-6 to a lesser extent and IL-1 weakly was suggested from LPS-stimulated $MK2^{-/-}$ spleenocytes where TNFα, IL-6, and IL-1β were inhibited 92%, 72% and 40%, respectively (Kotlyarov et al., 1999).

PF-3644022 is orally efficacious at inhibiting TNFα production in LPS-challenged rats and blocking paw swelling in the chronic SCW-arthritis model. Whereas p38 kinase inhibitors maximally inhibit TNFα production 100% in the rLPS model and 90-95% paw swelling in the rSCW model (Burnette et al., 2009; Hope et al., 2009), MK2 inhibitors are somewhat less efficacious. PF-3644022 inhibits up to 90% TNFα levels in rLPS and only 80% paw swelling in rSCW model. In the rSCW model, a p38 kinase inhibitor was shown to protect against inflammation-mediated joint and bone destruction (Burnette et al., 2009). Unfortunately, bone and cartilage histology were not measured in

our rSCW studies with PF-3644022. It would have been interesting to see if joint preservation was sufficient with MK2 inhibitor-mediated reductions in TNFα and IL-6 alone, especially since IL-1β has been implicated in bone and cartilage destruction in this model (Wilder et al., 1989).

In this report, we show excellent correlation that MK2 inhibition in cells is closely linked to TNFα inhibition in human cells and in rats, and to reduction of paw swelling in a chronic model of arthritis (Fig. 7). To achieve maximal efficacy in the rSCW model, we show that a C_{min} equivalent to at least the rLPS-TNFα EC_{50} must be maintained throughout dosing of PF-3644022 (Fig. 6). At a half-maximal response level, PF-3644022 total exposure in blood would be 1-11 μM (Table 5). However, if an EC_{80} exposure is needed in humans for RA efficacy, then PF-3644022 total blood levels would be 5-50 μM. Projected human doses based on the pharmacology described in this paper would be large, more than 300 mg twice a day (unpublished data). Given the biochemical inefficiency of MK2 as an anti-inflammatory target and the constant micromolar blood levels required for MK2 inhibition, sufficient kinase selectivity to establish an acceptable therapeutic index is challenging. That said, we continued developing PF-3644022 and evaluated its safety profile in rats, dogs and monkeys. While PF-3644022 is well tolerated in rats, acute hepatotoxicity is observed in dogs and monkeys at insufficient margins to continue developing PF-3644022. Similar toxicity is also observed with other molecules in the benzothiophene series suggesting that liver toxicity is likely scaffold- related (Daniels, J.S., personal communication).

8. ACKNOWLEDGMENTS

We thank Thomas L. Fevig, David L. Brown and Daniel R. Dukesherer for assistance in preparative scale-up of PF-3644022 and Po-Chang Chiang for compound milling to support in vivo animal model testing.

References

Anderson DR, Hegde S, Reinhard E, Gomez L, Vernier WF, Lee L, Liu S, Sambandam A, Snider PA and Masih L (2005) Aminocyanopyridine inhibitors of mitogen activated protein kinase-activated protein kinase 2 (MK-2). *Bioorg Med Chem Lett* **15**:1587-1590.

Anderson DR, Meyers MJ, Kurumbail RG, Caspers N, Poda GI, Long SA, Pierce BS, Mahoney MW and Mourey RJ (2009a) Benzothiophene inhibitors of MK2. Part 1: structure-activity relationships, assessments of selectivity and cellular potency. *Bioorg Med Chem Lett* **19**:4878-4881.

Anderson DR, Meyers MJ, Kurumbail RG, Caspers N, Poda GI, Long SA, Pierce BS, Mahoney MW, Mourey RJ and Parikh MD (2009b) Benzothiophene inhibitors of MK2. Part 2: improvements in kinase selectivity and cell potency. *Bioorg Med Chem Lett* **19**:4882-4884.

Anderson DR, Meyers MJ, Vernier WF, Mahoney MW, Kurumbail RG, Caspers N, Poda GI, Schindler JF, Reitz DB and Mourey RJ (2007) Pyrrolopyridine inhibitors of mitogen-activated protein kinase-activated protein kinase 2 (MK-2). *J Med Chem* **50**:2647-2654.

Burnette BL, Selness S, Devraj R, Jungbluth G, Kurumbail R, Stillwell L, Anderson G, Mnich S, Hirsch J, Compton R, De Ciechi P, Hope H, Hepperle M, Keith RH, Naing W, Shieh H, Portanova J, Zhang Y, Zhang J, Leimgruber RM and Monahan J (2009) SD0006: a potent, selective and orally available inhibitor of p38 kinase. *Pharmacology* **84**:42-60.

Card A, Caldwell C, Min H, Lokchander B, Hualin X, Sciabola S, Kamath AV, Clugston SL, Tschantz WR, Leyu W and Moshinsky DJ (2009) High-throughput biochemical kinase selectivity assays: panel development and screening applications. *J Biomol Screen* **14**:31-42.

Cheng R, Felicetti B, Palan S, Toogood-Johnson I, Scheich C, Barker J, Whittaker M and Hesterkamp T (2009) High-resolution crystal structure of human mapkap kinase 3 in complex with a high affinity ligand. *Protein Sci* **19**:168-173.

Dayer JM, Feige U, Edwards CK, 3rd and Burger D (2001) Anti-interleukin-1 therapy in rheumatic diseases. *Curr Opin Rheumatol* **13**:170-176.

Dominguez C, Powers DA and Tamayo N (2005) p38 MAP kinase inhibitors: many are made, but few are chosen. *Curr Opin Drug Discov Devel* **8**:421-430.

Gaestel M (2006) MAPKAP kinases - MKs - two's company, three's a crowd. *Nat Rev Mol Cell Biol* **7**:120-130.

Gaestel M, Kotlyarov A and Kracht M (2009) Targeting innate immunity protein kinase signalling in inflammation. *Nat Rev Drug Discov* **8**:480-499.

Gaestel M, Mengel A, Bothe U and Asadullah K (2007) Protein kinases as small molecule inhibitor targets in inflammation. *Curr Med Chem* **14**:2214-2234.

Goldberg DR, Choi Y, Cogan D, Corson M, DeLeon R, Gao A, Gruenbaum L, Hao MH, Joseph D, Kashem MA, Miller C, Moss N, Netherton MR, Pargellis CP, Pelletier J, Sellati R, Skow D, Torcellini C, Tseng YC, Wang J, Wasti R, Werneburg B, Wu JP and Xiong Z (2008) Pyrazinoindolone inhibitors of MAPKAP-K2. *Bioorg Med Chem Lett* **18**:938-941.

Hammaker D and Firestein GS (2010) "Go upstream, young man": lessons learned from the p38 saga. *Ann Rheum Dis* **69 Suppl 1**:i77-82.

Hegen M, Gaestel M, Nickerson-Nutter CL, Lin LL and Telliez JB (2006) MAPKAP kinase 2-deficient mice are resistant to collagen-induced arthritis. *J Immunol* **177**:1913-1917.

Hennigan S and Kavanaugh A (2008) Interleukin-6 inhibitors in the treatment of rheumatoid arthritis. *Ther Clin Risk Manag* **4**:767-775.

Hillig RC, Eberspaecher U, Monteclaro F, Huber M, Nguyen D, Mengel A, Muller-Tiemann B and Egner U (2007) Structural basis for a high affinity inhibitor bound to protein kinase MK2. *J Mol Biol* **369**:735-745.

Hope HR, Anderson GD, Burnette BL, Compton RP, Devraj RV, Hirsch JL, Keith RH, Li X, Mbalaviele G, Messing DM, Saabye MJ, Schindler JF, Selness SR, Stillwell LI, Webb EG, Zhang J and Monahan JB (2009) Anti-inflammatory properties of a novel N-phenyl pyridinone inhibitor of p38 mitogen-activated protein kinase: preclinical-to-clinical translation. *J Pharmacol Exp Ther* **331**:882-895.

Keminer O, Kraemer J, Kahmann J, Sternberger I, Scheich C, Jungmann J, Schaert S, Winkler D, Ichihara O, Whittaker M, Ullmann D and Hesterkamp T (2009) Novel MK2 inhibitors by fragment screening. *Comb Chem High Throughput Screen* **12**:697-703.

Kotlyarov A, Neininger A, Schubert C, Eckert R, Birchmeier C, Volk HD and Gaestel M (1999) MAPKAP kinase 2 is essential for LPS-induced TNF-alpha biosynthesis. *Nat Cell Biol* **1**:94-97.

Kuiper S, Joosten LA, Bendele AM, Edwards CK, 3rd, Arntz OJ, Helsen MM, Van de Loo FA and Van den Berg WB (1998) Different roles of tumour necrosis factor alpha and interleukin 1 in murine streptococcal cell wall arthritis. *Cytokine* **10**:690-702.

Leatherbarrow RJ (2001) *GraFit Version 5*. Erithacus Software Ltd., Horley, United Kingdom.

Lee JC, Laydon JT, McDonnell PC, Gallagher TF, Kumar S, Green D, McNulty D, Blumenthal MJ, Heys JR, Landvatter SW and et al. (1994) A protein kinase involved in the regulation of inflammatory cytokine biosynthesis. *Nature* **372**:739-746.

McInnes IB and Schett G (2007) Cytokines in the pathogenesis of rheumatoid arthritis. *Nat Rev Immunol* **7**:429-442.

Neininger A, Kontoyiannis D, Kotlyarov A, Winzen R, Eckert R, Volk HD, Holtmann H, Kollias G and Gaestel M (2002) MK2 targets AU-rich elements and regulates biosynthesis of tumor necrosis factor and interleukin-6 independently at different post-transcriptional levels. *J Biol Chem* **277**:3065-3068.

Pettus LH and Wurz RP (2008) Small molecule p38 MAP kinase inhibitors for the treatment of inflammatory diseases: novel structures and developments during 2006-2008. *Curr Top Med Chem* **8**:1452-1467.

Ronkina N, Kotlyarov A, Dittrich-Breiholz O, Kracht M, Hitti E, Milarski K, Askew R, Marusic S, Lin LL, Gaestel M and Telliez JB (2007) The mitogen-activated protein kinase (MAPK)-activated protein kinases MK2 and MK3 cooperate in

stimulation of tumor necrosis factor biosynthesis and stabilization of p38 MAPK. *Mol Cell Biol* **27**:170-181.

Schindler JF, Godbey A, Hood WF, Bolten SL, Broadus RM, Kasten TP, Cassely AJ, Hirsch JL, Merwood MA, Nagy MA, Fok KF, Saabye MJ, Morgan HM, Compton RP, Mourey RJ, Wittwer AJ and Monahan JB (2002) Examination of the kinetic mechanism of mitogen-activated protein kinase activated protein kinase-2. *Biochim Biophys Acta* **1598**:88-97.

Schindler JF, Monahan JB and Smith WG (2007) p38 pathway kinases as anti-inflammatory drug targets. *J Dent Res* **86**:800-811.

Schlapbach A, Feifel R, Hawtin S, Heng R, Koch G, Moebitz H, Revesz L, Scheufler C, Velcicky J, Waelchli R and Huppertz C (2008) Pyrrolo-pyrimidones: a novel class of MK2 inhibitors with potent cellular activity. *Bioorg Med Chem Lett* **18**:6142-6146.

Scott DL and Kingsley GH (2006) Tumor necrosis factor inhibitors for rheumatoid arthritis. *N Engl J Med* **355**:704-712.

Shi Y, Kotlyarov A, Laabeta K, Gruber AD, Butt E, Marcus K, Meyer HE, Friedrich A, Volk HD and Gaestel M (2003) Elimination of protein kinase MK5/PRAK activity by targeted homologous recombination. *Mol Cell Biol* **23**:7732-7741.

Smith PA, Tripp BC, DiBlasio-Smith EA, Lu Z, LaVallie ER and McCoy JM (1998) A plasmid expression system for quantitative in vivo biotinylation of thioredoxin fusion proteins in Escherichia coli. *Nucleic Acids Res* **26**:1414-1420.

Smolen JS and Steiner G (2003) Therapeutic strategies for rheumatoid arthritis. *Nat Rev Drug Discov* **2**:473-488.

Swinney DC (2004) Biochemical mechanisms of drug action: what does it take for success? *Nat Rev Drug Discov* **3**:801-808.

Trujillo JI, Meyers MJ, Anderson DR, Hegde S, Mahoney MW, Vernier WF, Buchler IP, Wu KK, Yang S, Hartmann SJ and Reitz DB (2007) Novel tetrahydro-beta-carboline-1-carboxylic acids as inhibitors of mitogen activated protein kinase-activated protein kinase 2 (MK-2). *Bioorg Med Chem Lett* **17**:4657-4663.

Wilder RL, Lafyatis R, Yocum DE, Case JP, Kumkumian GK and Remmers EF (1989) Mechanisms of bone and cartilage destruction in rheumatoid arthritis: lessons from the streptococcal cell wall arthritis model in LEW/N rats. *Clin Exp Rheumatol* **7 Suppl 3**:S123-127.

Winzen R, Kracht M, Ritter B, Wilhelm A, Chen CY, Shyu AB, Muller M, Gaestel M, Resch K and Holtmann H (1999) The p38 MAP kinase pathway signals for cytokine-induced mRNA stabilization via MAP kinase-activated protein kinase 2 and an AU-rich region-targeted mechanism. *EMBO J* **18**:4969-4980.

Wu JP, Wang J, Abeywardane A, Andersen D, Emmanuel M, Gautschi E, Goldberg DR, Kashem MA, Lukas S, Mao W, Martin L, Morwick T, Moss N, Pargellis C, Patel UR, Patnaude L, Peet GW, Skow D, Snow RJ, Ward Y, Werneburg B and White A (2007) The discovery of carboline analogs as potent MAPKAP-K2 inhibitors. *Bioorg Med Chem Lett* **17**:4664-4669.

Xiong Z, Gao DA, Cogan DA, Goldberg DR, Hao MH, Moss N, Pack E, Pargellis C, Skow D, Trieselmann T, Werneburg B and White A (2008) Synthesis and SAR studies of indole-based MK2 inhibitors. *Bioorg Med Chem Lett* **18**:1994-1999.

10. Footnotes

This study was sponsored by Pfizer Inc.

Portions of this work were presented at the following conference: Daniels, J.S., Lai, Y., Davis, J.W., South, S.A., Stevens, J.C., Mourey, R.J., and Anderson, D.R. (2008) Inhibition of hepatobiliary transporters by a novel kinase inhibitor contributes to liver toxicity in nonclinical species. *Great Lakes Drug Metabolism Discussion Group*; 2008 May 1-2; Indianapolis, Indiana.

The person to who reprint requests should be addressed.

Dr. David R. Anderson

Pfizer Global Research & Development

Eastern Point Road

Groton, CT 06340

Email: david.r.anderson@pfizer.com

11. Legends for Figures

Fig. 1. Structure of PF-3644022

Fig. 2. Competitive inhibition pattern for PF-3644022 versus recombinant MK2 enzyme. Initial velocities were obtained with ATP as the varied substrate (0.625, 1.25, 2.5, 5, 10, 20 μM). The FITC-HSP27 peptide concentration was held constant at 500 nM. The concentrations of PF-3644022 used were 0 (inverted open triangles), 1.6 (filled triangles), 3.1 (open triangles), 6.2 (filled squares), 12.5 (open squares), 25 (filled circles) and 50 (open circles) nM. A, nonlinear fit of data (duplicate data points) to a competitive inhibition model using GraFit 5.0. B, Lineweaver-Burk double reciprocal plot of the data shown in Fig. 1A. The enzymatic competitive inhibition constant for PF-364022 in this representative experiment is 2.72 +/- 0.11 nM (S.E.).

Fig. 3. PF-3644022 inhibition of MK2 activity and TNFα inhibition in LPS-stimulated U937 cells, human PBMCs and HWB. A, inhibition of MK2 activity (p-Ser78-HSP27), phospho-JNK, phospho-p38 MAPK kinases and TNFα production in U937 cells at increasing concentrations of PF-3644022. U937 cells were stimulated with 100 ng/ml LPS for 30 min and then cell lysates prepared as described in *Methods*. Lysate proteins were resolved by SDS-PAGE and HSP27, p38 and JNK total and phospho-specific protein levels detected by Western blotting. Immunoreactivity levels were quantitated using fluorescently-tagged

secondary antibodies and LiCor scanning. The ratio of phospho- to total target protein was plotted versus PF-3644022 concentration with 100% control defined as LPS-stimulated signal without compound. TNFα levels in the culture supernatant were measured 4 h after LPS-stimulation as described in *Methods*. Data points shown are representative of a single experiment repeated three times. Non-linear regression of the data using a 4-parameter fit generated TNFα and p-HSP27 IC_{50} values of 0.19 +/- 0.04 nM and 0.27 +/- 0.08 nM (S.E.), respectively. B, PF-3644022 inhibition of LPS-stimulated TNFα production in U937 cells, human PBMCs and HWB relative to MK2 enzyme inhibition. Concentration response for PF-3644022 inhibition of TNFα levels in culture media or in plasma from U937 cells, hPBMCs or HWB stimulated with 100 ng/ml LPS for 4 h is shown. Inhibition of MK2 enzyme by PF-3644022 was determined in the MK2 Caliper assay as described in *Methods*. Curves were generated using 4-parameter non-linear regression of data points (mean +/- S.E.M.) from three separate experiments (in duplicate). Calculated IC_{50} values for MK2 and TNFα inhibition by PF-3644022 are: MK2 (9.0 +/- 0.4 nM), U937 (142 +/- 19 nM), hPBMC (214 +/- 49 nM), HWB (1376 +/- 434 nM).

Fig. 4. Dose-dependent inhibition of LPS-induced inflammatory cytokines in human PBMCs (A) and HWB (B) treated with PF-3644022. Following stimulation of isolated hPBMCs in culture or HWB ex vivo with 100 ng/ml LPS, TNFα (closed circles) or IL-1β (open circles), IL-6 (closed squares), and IL-8 (open squares) levels were measured at 4 or 16 h, respectively, and quantitated from culture

media or human plasma using a MSD multiplex human cytokine assay kit. Data points shown are mean values (+/- S.E.M.) from two independent experiments (in duplicate) using three separate blood donors for both (A) and (B). Curves were generated using 4-parameter non-linear regression of the data points and IC_{50} values for cytokine inhibition in (A) are TNFα (0.214 +/- 0. 049 μM), IL-1β (2.71 +/- 0.64 μM), IL-6 (1.40 +/- 0.18 μM), IL-8 (2.59 +/- 0.70 μM); and in (B) are TNFα (1.38 +/- 0.43 μM), IL-1β (>20 μM), IL-6 (12.7 +/- 1.0 μM), IL-8 (>20 μM).

Fig. 5. Effect of PF-3644022 on LPS-induced TNFα production in rats as a function of dose (A), total plasma concentration (B) and pharmacokinetic-pharmacodynamic (PK-PD) response (C). Adult male Lewis rats (~225-250 g, 5 rats/group) were orally dosed with PF-3644022 suspension or vehicle (0.5% methylcellulose, 0.025% Tween 20) 4 h prior to i.v. administration of 1 mg/kg LPS. Blood was collected 90 min after LPS challenge and serum TNFα levels determined by ELISA. Compound blood levels were quantitated by LC-MS/MS. Three independent experiments were run dosing 0.2, 0.6, 2, 6, 20 and 60 mg/kg PF-3644022. Mean (+/- S.E.M.) data from all three experiments are plotted for dose-response (A) and concentration-response (B). Curves were generated using 4-parameter non-linear regression of the data points and ED_{50}, ED_{80}, EC_{50} and EC_{80} values are shown in Table 5. In a PK-PD study of PF-3644022 in LPS-challenged rats, three independent experiments were run (5 animals/group) using an ~ED_{80} oral dose (20 mg/kg) of PF-3644022 for various time points (0, 0.5, 1, 2, 4, 8, 12,

24, 36 h) prior to i.v. challenge by LPS (1 mg/kg). Blood was collected 90 min later and analyzed for TNFα (closed circles) and PF-3644022 (open circles) levels as described above. Mean values (+/- S.E.M.) from three experiments for TNFα levels and PF-3644022 concentration in blood over time are shown in (C).

Fig. 6. PF-3644022 dose-dependently reduces paw inflammation in the rat SCW-induced arthritis model. PF-3644022 was administered orally twice daily from days 10 to 21, then hind paw volumes measured and blood collected at various times on day 21 after the last dose for determination of compound levels in plasma as described in *Methods*. Mean values of animal groups (4-8 female Lewis rats/group) from three separate experiments are plotted as percent inhibition of paw swelling versus dose (A). The concentration of PF-3644022 in plasma over time was determined using 3 rats per dose after the last dose of PF-3644022 in experiment #3 (B). ED_{50}, EC_{50}, C_{max}, C_{min} and AUC values calculated from this study are reported in Table 5.

Fig. 7. PF-3644022 pharmacologic profile links MK2 inhibition with inhibition of TNFα production in human cells and blood, and efficacy in rat acute and chronic models of inflammation. A plot of response versus PF-3644022 concentration summarizes data from several studies in this report: concentration to inhibit LPS-stimulated p-HSP27 and TNFα production in U937 cells (Fig. 3A) and hPBMCs (Fig. 3B), unbound plasma concentration or free fraction (ff) of PF-3644022 in HWB for TNFα inhibition (Fig 4B), concentration (ff at 5.5 hr) in the acute LPS-

JPET Fast Forward. Published on March 17, 2010 as DOI: 10.1124/jpet.110.166173
This article has not been copyedited and formatted. The final version may differ from this version.

challenged rat TNFα model (Fig. 5B), and inhibition of paw swelling (C_{min} ff) from the chronic SCW-induced rat arthritis model (Fig. 6B). A 4-parameter non-linear regression fit of the data indicates a collective $EC_{50} = 0.139$, $r^2 = 0.81$.

JPET Fast Forward. Published on March 17, 2010 as DOI: 10.1124/jpet.110.166173
This article has not been copyedited and formatted. The final version may differ from this version.

12. Tables

TABLE 1

Inhibitory properties of PF-3644022 against recombinant MK2 enzyme and other MAPKAP kinase family members

MK2 IC_{50} (nM)	5.2 +/- 1.9 (n=13)
MK2 K_i (nM)	3.0 +/- 1.0 (n=6)
MK2 binding K_d (nM)	5.9 +/- 3.8 (n=3)
k_{on} ($M^{-1}s^{-1}$)	2.1e6 +/- 0.3e6
k_{off} (s^{-1})	1.26 +/- 0.17
$t_{1/2}$ (s)	146 +/- 51
MAPKAP kinases IC_{50} (nM):	
MK3	53
PRAK	5
MNK1	3000
MNK2	148
MSK1/2	>1000
RSK1/2/3/4	>1000

Data are expressed as mean values +/- S.E.M. for multiple independent experiments as indicated by “n” or for duplicate experiments with MAPKAP kinase family members.

JPET Fast Forward. Published on March 17, 2010 as DOI: 10.1124/jpet.110.166173
This article has not been copyedited and formatted. The final version may differ from this version.

TABLE 2

Kinase selectivity profile of PF-3644022

IC_{50} values are shown for the kinases that were inhibited >50% at 1 μM PF-3644022 against a 200 human kinase selectivity panel (see supplemental section Table 1).

Kinase	Group	IC_{50} (nM)	Selectivity[a] (-fold)
MK2	CAMK	5	-
AMPK	CAMK	117	23
BrSK1	CAMK	187	37
BrSK2	CAMK	90	18
CaMKII	CAMK	70	14
DRAK1	CAMK	71	14
MK3	CAMK	53	10
MNK2	CAMK	148	30
PhKγ2	CAMK	528	106
Pim1	CAMK	88	18
PRAK	CAMK	5	1
CDK1/cycB	CMGC	354	71
CDK5/p35	CMGC	902	180
ASK1	STE	60	12
Axl	TK	428	86

JPET Fast Forward. Published on March 17, 2010 as DOI: 10.1124/jpet.110.166173
This article has not been copyedited and formatted. The final version may differ from this version.

Mer	TK	76	15
RIPK2	TKL	590	118

[a]Fold selectivity was relative to MK2 IC_{50} value.

AMPK, AMP-activated protein kinase; BrSK1, brain Ser/Thr kinase 1; BrSK2, brain Ser/Thr kinase 2; CaMKII, calcium/calmodulin-dependent protein kinase type II; DRAK1, DAP kinase-related apoptosis-inducing protein kinase 1; MK3, MAPKAP kinase 3; MNK2, MAPK-interacting kinase 2; PhKγ2, phosphorylase kinase testis/liver gamma 2; PRAK, p38-regulated/activated kinase; CDK1/cycB, cyclin-dependent kinase 1/cyclin B complex; CDK5/p35, cyclin-dependent kinase 5/p35 complex; ASK1, apoptosis signal-regulating kinase 1; RIPK2, receptor-interacting protein kinase 2.

JPET Fast Forward. Published on March 17, 2010 as DOI: 10.1124/jpet.110.166173
This article has not been copyedited and formatted. The final version may differ from this version.

TABLE 3

PF-3644022 inhibition of LPS-induced MK2 activity and cytokine production in human cells and whole blood.

Assay	IC_{50} (μM) +/- SEM
U937- TNFα	0.159 +/- 0.014
U937 MK2 activity	0.201 +/- 0.042
hPBMC- TNFα	0.160 +/- 0.069
hPBMC- IL-1β	2.78 +/- 0.51
hPBMC- IL-6	1.26 +/- 0.17
hPBMC- IL-8	2.09 +/- 0.51
HWB- TNFα	1.97 +/- 0.80
HWB MK2 activity	1.60 +/- 0.53
HWB- IL-1β	> 25
HWB- IL-6	10.3 +/- 2.33
HWB- IL-8	> 25

Data are expressed as mean values +/- S.E.M. for multiple independent experiments as follows: U937 TNFα (n=8), U937 MK2 activity (n=5), hPBMC cytokines (n=4), HWB MK2 activity (n=3), and HWB cytokines (n=6). For hPBMC and HWB studies, each independent experiment represents an individual blood donor.

JPET Fast Forward. Published on March 17, 2010 as DOI: 10.1124/jpet.110.166173
This article has not been copyedited and formatted. The final version may differ from this version.

TABLE 4

Pharmacokinetic parameters of MK2 inhibitors in Sprague-Dawley Rats

	Clp[a]	Vd_{ss}	$t_{1/2}$	C_{max}[b]	T_{max}	$AUC_{0-\infty}$[b]	F
	L/hr/kg	*L/kg*	*hr*	*μM*	*hr*	*μM*hr*	*%*
PF-3644022	0.62	1.5	9.1	0.66	0.17	1.8	46

[a]1 mpk parenteral administration, n=2

[b]3 mpk oral administration, n=3

JPET Fast Forward. Published on March 17, 2010 as DOI: 10.1124/jpet.110.166173
This article has not been copyedited and formatted. The final version may differ from this version.

TABLE 5

In vivo efficacy of PF-3644022 in rat acute and chronic inflammation models

Acute LPS-induced TNFα production	
ED_{50}/ED_{80} (mg/kg)	6.9/19
EC_{50}/EC_{80} ($C_{5.5hr}$; μM)	1.4/4.2
EC_{50}/EC_{80} ff[a] ($C_{5.5hr}$; μM)	0.11/0.34
Chronic SCW-induced arthritis	
ED_{50}/ED_{80} (mg/kg, b.i.d.)	20/50-100[b]
EC_{50}/EC_{80} (C_{max}; μM)	11/28-51[b]
EC_{50}/EC_{80} (C_{min}; μM)	0.91/4.9-13.5[b]
EC_{50}/EC_{80} (AUC; μM*hr)	34/117-248[b]

[a]Free fraction concentrations of PF-3644022 were calculated from a measured PF-3644022 rat plasma protein value of 92.1%.

[b]Efficacy values at 80% inhibition are approximate due to maximum efficacy of 75-82% observed with MK2 inhibitors in the rat SCW model.

LPS-induced TNFα production $ED_{50/80}$ and $EC_{50/80}$ values from the rat acute model were calculated from data shown in Fig. 5A and 5B, respectively. $ED_{50/80}$ and $EC_{50/80}$ parameters from the rat SCW-induced arthritis model were determined using data from Fig. 6A and 6B, respectively.

Figure 1

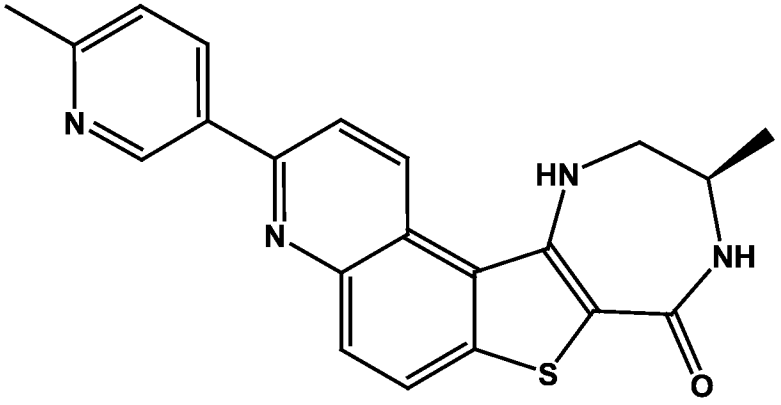

Figure 2

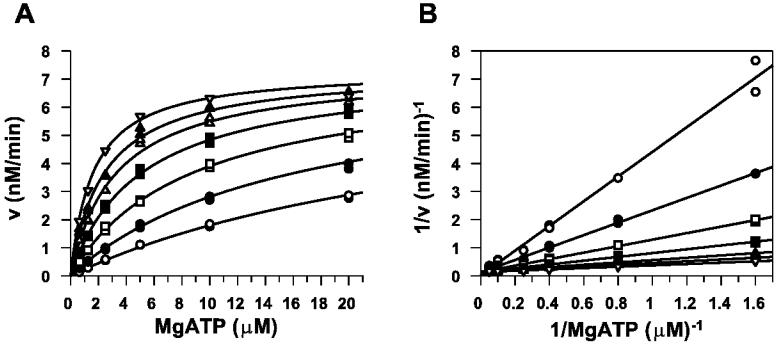
A
v (nM/min)
0
1
2
3
4
5
6
7
8
0 2 4 6 8 10 12 14 16 18 20
MgATP (μM)
B
1/v (nM/min)-1
0
1
2
3
4
5
6
7
8
0 0.2 0.4 0.6 0.8 1 1.2 1.4 1.6
1/MgATP (μM)-1

Figure 3

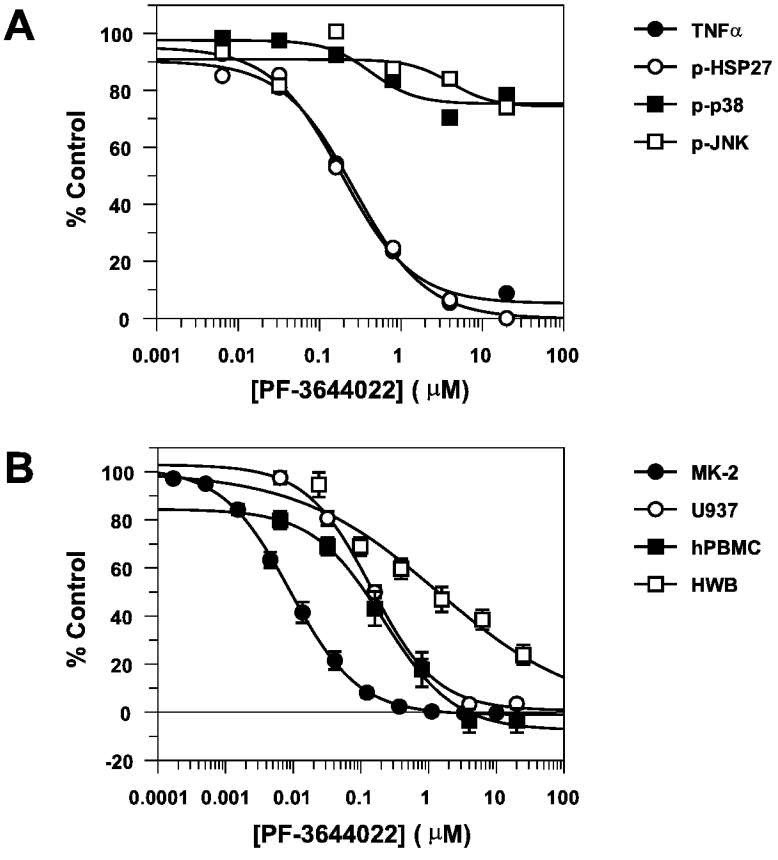
A
100
80
60
40
20
0
% Control
0.001
0.01
0.1
1
10
100
[PF-3644022] (μM)
TNFα
p-HSP27
p-p38
p-JNK
B
100
80
60
40
20
0
-20
% Control
0.0001
0.001
0.01
0.1
1
10
100
[PF-3644022] (μM)
MK-2
U937
hPBMC
HWB

Figure 4

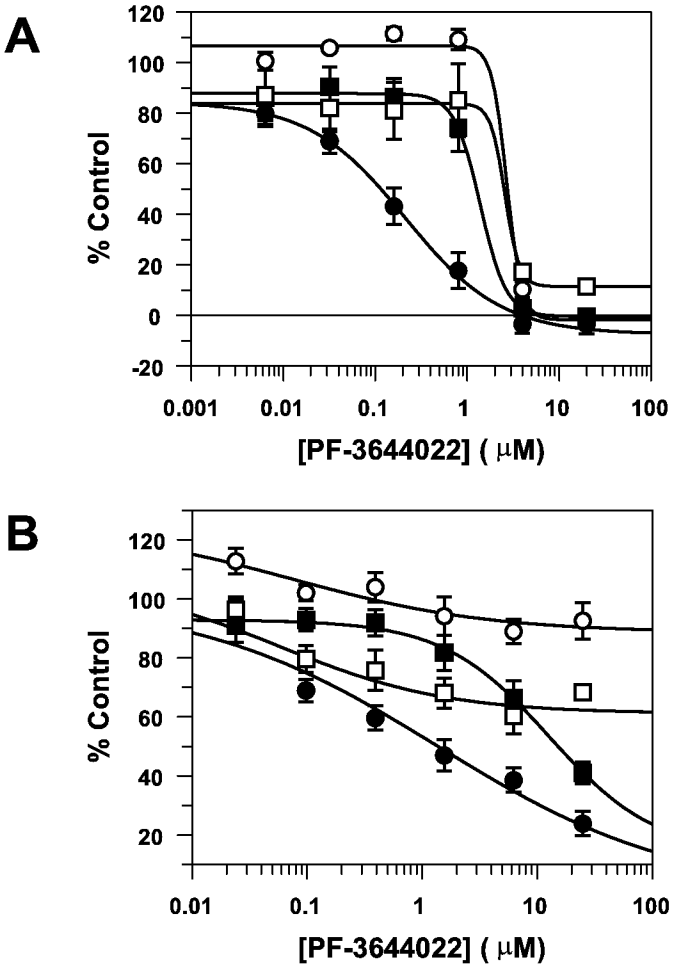
A
120
100
80
60
40
20
0
-20
% Control
0.001
0.01
0.1
1
10
100
[PF-3644022] (μM)
B
120
100
80
60
40
20
% Control
0.01
0.1
1
10
100
[PF-3644022] (μM)

Figure 5

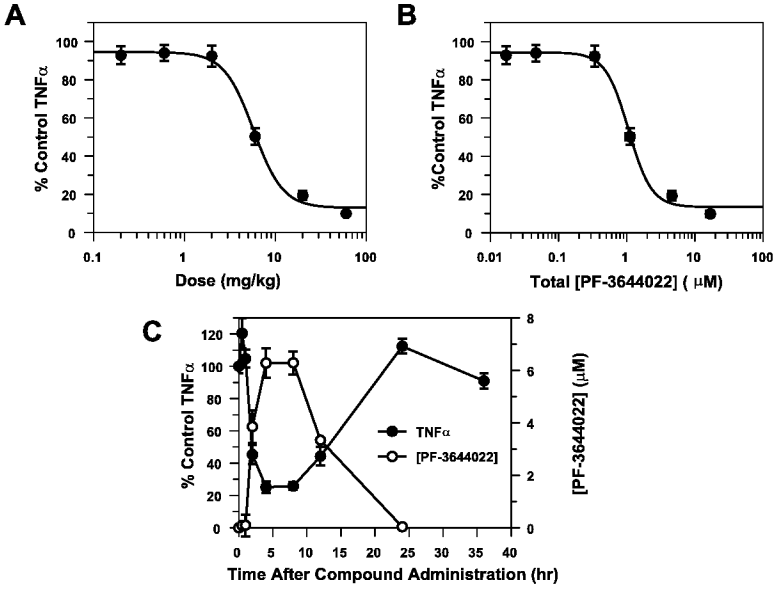
A
% Control TNFα
Dose (mg/kg)
B
%Control TNFα
Total [PF-3644022] (μM)
C
% Control TNFα
[PF-3644022] (μM)
TNFα
[PF-3644022]
Time After Compound Administration (hr)

Figure 6

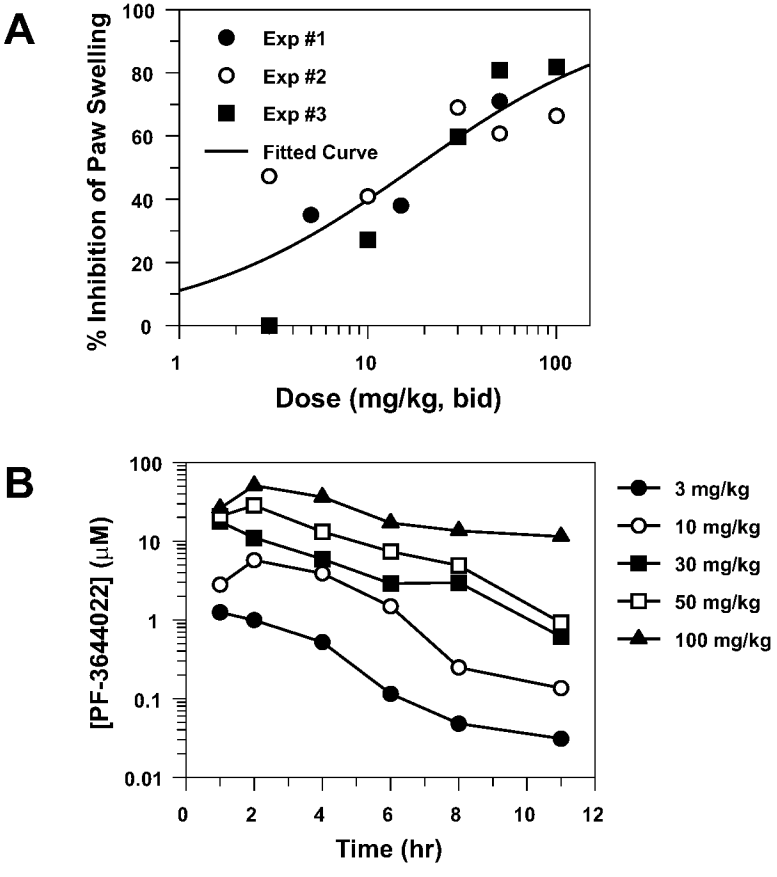
A
% Inhibition of Paw Swelling
Exp #1
Exp #2
Exp #3
Fitted Curve
Dose (mg/kg, bid)
B
[PF-3644022] (μM)
Time (hr)
3 mg/kg
10 mg/kg
30 mg/kg
50 mg/kg
100 mg/kg

Figure 7

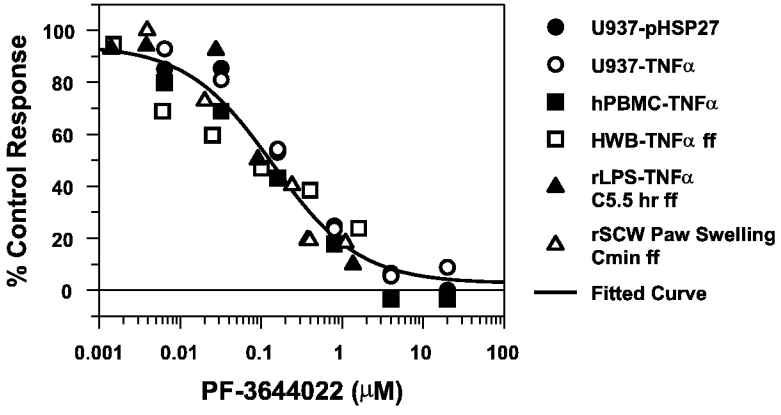
% Control Response
100
80
60
40
20
0
0.001
0.01
0.1
1
10
100
PF-3644022 (μM)
U937-pHSP27
U937-TNFα
hPBMC-TNFα
HWB-TNFα ff
rLPS-TNFα
C5.5 hr ff
rSCW Paw Swelling
Cmin ff
Fitted Curve